PLP/SEC/NMR Study of Free Radical Copolymerization of Styrene and Glycidyl Methacrylate

Wei Wang and Robin A. Hutchinson*

Department of Chemical Engineering, Dupuis Hall, Queen's University, Kingston, Ontario K7L 3N6, Canada

Received June 27, 2008; Revised Manuscript Received October 2, 2008

ABSTRACT: Free radical copolymerization of glycidyl methacrylate (GMA) and styrene (ST) is systematically investigated using low conversion pulsed laser polymerization (PLP) experiments. It is shown that GMA, like other methacrylate monomers, undergoes significant depropagation at elevated temperatures. While ST/GMA copolymer composition is well represented by the terminal model, the copolymer-averaged propagation rate coefficient for the system is not; the latter quantity is represented using the implicit penultimate unit model. The PLP data are used to estimate GMA depropagation kinetics as well as ST/GMA monomer ($r_{ST} = 0.31$ and $r_{GMA} = 0.51$) and radical ($s_{ST} = 0.28$ and $s_{GMA} = 1.05$) reactivity ratios, which show no significant variation in the 50−140 °C temperature range examined. The GMA/ST copolymerization behavior is compared to that of butyl methacrylate (BMA) with ST; GMA monomer is more active toward styrene radicals than BMA, and a GMA unit in the penultimate position of styrene radicals reduces copolymerization propagation to a greater extent.

Introduction

Copolymers of methacrylates and styrene (ST) are used as binder resins in automotive coatings because of their excellent chemical and mechanical properties. Due to the need to reduce the volatile organic content of coating formulations, conventional solvent-borne resins have been replaced by high solids resins consisting of low molecular weight (MW) polymers with reactive functionality, produced at high temperature using a semibatch starved-feed policy.[1] These oligomeric chains form a high MW polymer network on the surface to be coated via reaction of the functional groups with an added cross-linking agent. Sufficient functional monomers (e.g., glycidyl methacrylate (GMA)) must be included in the resin recipe to ensure that almost all of the chains participate in the cross-linking reactions.

To tailor acrylic resin properties and their manufacturing process, it is necessary to improve the understanding of the free-radical copolymerization mechanisms and kinetics under these higher temperature (>120 °C) conditions. Methacrylate depropagation and penultimate chain growth are two important effects that must be considered, as discussed in our previous study of the copolymerization kinetics of ST with butyl methacrylate (BMA).[2] The mechanistic model and set of measured rate coefficients provided a good description of a set of starved-feed ST/BMA semibatch copolymerization experiments conducted at conditions mimicking industrial production.[3] The same model structure was used to describe similar copolymerizations of ST with dodecyl methacrylate (DMA),[4] with ST/DMA copolymerization rate coefficients taken from previous literature. To further extend this modeling effort, we now turn our attention to copolymerization of ST with GMA, a monomer commonly used to introduce epoxy cross-linking sites to acrylic resins.[5,6] As described below, however, there is little data regarding GMA depropagation and high temperature copolymerization behavior. This study rectifies this deficiency, using pulsed laser polymerization (PLP) techniques to study the kinetics.

Methacrylates have been known to depropagate at high temperatures ever since Bywater's investigation of methyl methacrylate indicated that the polymerization equilibrates at a certain monomer concentration for a given temperature and does not proceed when the initial monomer concentration is below this equilibrium value.[7] Free-radical depropagation kinetics of several methacrylates (but not GMA) was studied by Hutchinson et al.,[8] using PLP coupled with size exclusion chromatography (SEC) to measure an effective propagation rate coefficient as a function of temperature. Methacrylates undergo appreciable rates of depropagation (reversible chain growth) under low monomer concentrations at temperatures greater than 120 °C

$$P_n^\bullet + M \underset{k_{dep}}{\overset{k_p}{\rightleftarrows}} P_{n+1}^\bullet \tag{1}$$

where $P_n^\bullet$ represents a growing radical of length n and M the monomer, and k_p and k_{dep} are the propagation and depropagation rate coefficients, respectively. The *effective* forward propagation rate coefficient, denoted here by k_p^{eff}, is given by

$$k_p^{eff} = k_p - k_{dep}/[M] \tag{2}$$

where k_p^{eff}, directly measured from PLP/SEC experiments, is a function of temperature and of the monomer concentration, $[M]$. Depropagation has a significant effect on the copolymer composition and the effective propagation kinetics when methacrylates copolymerize with other monomers.[9] Thus, knowledge of the GMA depropagation behavior seems essential when considering ST/GMA copolymerization kinetics.

The instantaneous copolymer composition (F_i^{inst}) is adequately represented by the well-known Mayo−Lewis equation

$$F_1^{inst} = \frac{r_1 f_1^2 + f_1 f_2}{r_1 f_1^2 + 2 f_1 f_2 + r_2 f_2^2} \tag{3}$$

for ST/methacrylate copolymerizations, where f_i is the mole fraction of monomer i (e.g., $f_1 = [M_1]/([M_1] + [M_2])$), and monomer reactivity ratios r_1 and r_2 are defined as k_{p11}/k_{p12} and k_{p22}/k_{p21}. The monomer reactivity ratios for ST/GMA free radical copolymerization reported by several research groups[10−14] are not consistent, as summarized in Table 1. A second goal of this work, thus, is to determine reasonable values for ST/GMA reactivity ratios, and to examine whether these values vary with temperature. Wolf et al.[11] reported a small but significant temperature dependence for ST/GMA between 110−160 °C, whereas no temperature dependence was found for ST/BMA between 50−150 °C.[2]

* To whom correspondence should be addressed. E-mail: robin.hutchinson@chee.queensu.ca.

10.1021/ma801435t CCC: $40.75
Published on Web 11/07/2008

Table 1. Literature Monomer Reactivity Ratios (r_{ST} and r_{GMA}) for the Free Radical Copolymerization of Styrene (ST) with Glycidyl Methacrylate (GMA)

	Dhal[10]	Wolf et al.[11]	Brar et al.[12]	Soundararajan et al.[13]	Beuermann et al.[14]
r_{ST}	0.36	0.20	0.48	0.53	0.29
r_{GMA}	0.65	0.64	0.60	0.45	0.48

While copolymer composition is well described by the terminal model, the copolymer-averaged propagation rate coefficient ($k_{p,cop}$) for many common systems is not. Measured $k_{p,cop}$ values by the PLP/SEC technique can be higher or lower than the terminal model predictions, with the deviation substantial in some cases.[4,15] The "implicit penultimate unit effect (IPUE)" model, which assumes that both terminal and penultimate units affect free-radical reactivity but selectivity is only determined by the terminal unit, provides a good representation for this behavior.[15] As the penultimate unit does not affect the selectivity of the radical, only a single pair of monomer reactivity ratios is required, namely $r_{11} = r_{21} = r_1$ and $r_{22} = r_{12} = r_2$. The IPUE model introduces radical reactivity ratios s_1 and s_2 ($s_i = k_{pjii}/k_{piii}$) and the expression for $k_{p,cop}$ is[15]

$$k_{p,cop} = \frac{r_1 f_1^2 + 2 f_1 f_2 + r_2 f_2^2}{[r_1 f_1/\bar{k}_{11}] + [r_2 f_2/\bar{k}_{22}]} \quad (4)$$

where $\bar{k}_{ii}$ values are dependent on monomer composition, homopropagation rate coefficients k_{piii}, and monomer and radical reactivity ratios according to eq 5.

$$\bar{k}_{11} = \frac{k_{p111}[r_1 f_1 + f_2]}{r_1 f_1 + [f_2/s_1]} \quad \bar{k}_{22} = \frac{k_{p222}[r_2 f_2 + f_1]}{r_2 f_2 + [f_1/s_2]} \quad (5)$$

It must be noted that the IPUE model is not the only one capable of representing $k_{p,cop}$ trends.[15] Furthermore, the ability of the terminal model to adequately describe copolymer composition data does not rule out the absence of explicit penultimate unit effects.[16] In most cases, however, the IPUE model provides an excellent simultaneous representation of copolymer composition and $k_{p,cop}$ data.[17−19] We have recently estimated radical reactivity ratios for ST/BMA copolymerization by fitting the IPUE model to experimentally determined $k_{p,cop}$ values measured by PLP/SEC experiments; it was found, as for monomer reactivity ratios, that the variation with temperature was insignificant.[2] To date, no studies of penultimate chain-growth kinetics have been reported for functional monomers such as GMA.

Both GMA depropagation kinetics and GMA/ST copolymerization chain growth kinetics can be studied using the PLP/SEC technique, which has proven to be a very simple and robust experimental technique for determining k_p (also k_p^{eff} and $k_{p,cop}$) and its temperature dependence while making very few assumptions, provided adequate care is taken with SEC analysis of polymer molecular weight distributions (MWDs).[20,21] The theoretical and practical aspects of the PLP/SEC technique have been discussed in detail in several reviews.[22−26] In PLP experiments, a mixture of monomer and photoinitiator is exposed to successive laser pulses at a constant repetition rate, usually between 10 and 100 Hz. Initiation of new chains occurs at each laser flash; these chains propagate and terminate in the dark period between pulses, with the radical concentration and the rate of termination decreasing with time. Growing macroradicals that escape termination all have the same chain length which increases linearly with time. There is a high probability that these surviving radicals are terminated at the next laser flash, which generates a new population of short radicals. Thus, a significant fraction of dead chains formed has a chain length L_0 corresponding to a chain lifetime equal to the time between pulses, t_0 (eq 6).

$$L_0 = k_p[M]t_0 \quad (6)$$

Because radicals have a certain probability of surviving the laser flash and of terminating at a later laser flash, the polymers with chain length of L_i ($=i \times L_0$; $i = 2, 3,...$) will also be formed. Good PLP structure, namely, clear primary and secondary inflection points in the first-derivative curves of the MWD with the position of the secondary inflection point at twice the value of the primary, is an important consistency check for analysis.

In this work, low conversion PLP experiments were carried out to investigate GMA depropagation kinetics at elevated temperatures and ST/GMA copolymerization behavior over a wide range of temperatures. The monomer reactivity ratios were determined by analyzing the proton NMR spectra of the copolymers and the radical reactivity ratios were estimated by nonlinear fitting of the IPUE model to $k_{p,cop}$ data using the commercial software Predici. Comparison of ST/BMA and ST/GMA systems was conducted to achieve a better understanding of the general copolymerization behavior of ST with methacrylates.

Experimental Section

GMA with 100 ppm of 4-methoxyphenol (97% purity), and styrene (99% purity) inhibited with 10−15 ppm of 4-*tert*-butylcatechol were purchased from Sigma Aldrich and used as received. The photoinitiator DMPA (2,2-dimethoxy-2-phenylacetophenone, 99% purity) and a xylene isomeric mixture with boiling point range between 136−140 °C were obtained from Sigma Aldrich and used as received. Chloroform-*d* with 99.96 atom %D was from Sigma Aldrich and used as received.

Low-conversion GMA homopolymerizations and ST/GMA copolymerizations were conducted in a pulsed laser setup consisting of a Spectra-Physics Quanta-Ray 100 Hz Nd: YAG laser that is capable of producing a 355 nm laser pulse of duration 7−10 ns and energy of 1−50 mJ per pulse. The laser beam is reflected twice (180°) to shine into a cylindrical quartz sample cell used as the PLP reactor. A digital delay generator (DDG, Stanford Instruments) is attached to the laser to regulate the pulse output repetition rate at a value between 10 and 100 Hz. Monomer mixtures in bulk or xylene solution with 3−5 mmol·L^{-1} DMPA photoinitiator were added to a quartz cell and exposed to laser energy, with temperature controlled by a circulating oil bath. Experiments were run in the temperature range of 50−175 °C at 20 Hz, with GMA mole fraction in the monomer mixture varied between 0−100%. Temperature was monitored during laser pulsing, and never increased more than 0.5 °C during polymerization. Monomer conversions were controlled below 3% to avoid significant composition drift; a few of the highest temperature experiments went to slightly higher conversion.

The composition of copolymers produced by PLP experiments were analyzed by proton NMR. The resulting samples were precipitated in methanol, redissolved in THF and reprecipitated twice, and dried in a vacuum oven at 60 °C. The polymer was then dissolved in chloroform-*d* for ^{1}H NMR analysis conducted at room temperature on a 400 MHz Bruker instrument. Typical NMR spectra of poly(ST), poly(GMA), and copolymer and the assignments of their resonances are shown in Figure S1, Supporting Information. The copolymer shows chemical shifts from the phenyl protons in the region of 6.6−7.3 ppm, and from the methyleneoxy (-OCH$_2$-) protons and methyl protons of GMA units in the region of 3.5−4.5 and 0.5−1.2 ppm, respectively. The remainder of the NMR spectra contains signals for protons in the copolymer methane, methylene, and epoxy groups.[12] Copolymer composition was estimated from ^{1}H NMR via three methods. For the first, the peak area from the phenyl protons is taken as 5ST, while the remainder of the spectrum is integrated to yield the remaining (3ST+10GMA) protons. This ratio was used to calculate the molar percentage of GMA units in the copolymer. For the second, the mole fraction of GMA in the copolymer was calculated according to $F_1 = 5\,A_1/(5\,A_1 + 2\,A_2)$, where A_1 and A_2 are the peak areas of the methyleneoxy and phenyl protons, respectively. For the third, the mole fraction

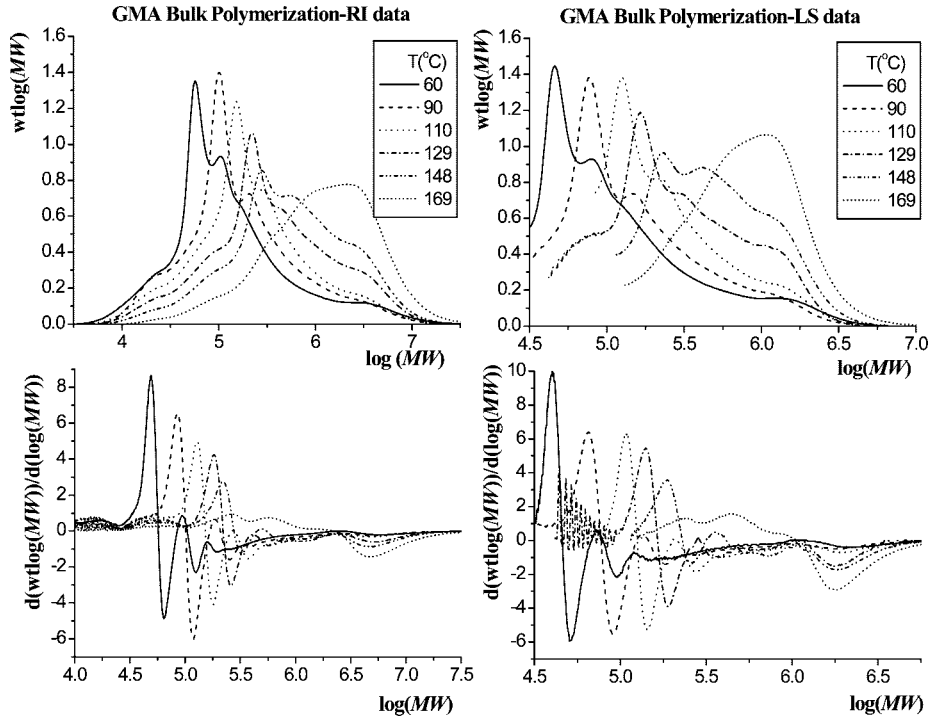

Figure 1. Molecular weight distributions (top) and corresponding first derivative (bottom) plots obtained for glycidyl methacrylate (GMA) homopolymer produced in bulk by pulsed laser polymerization at 20 Hz with temperatures from 60 to 169 °C, as measured by differential refractometer (DRI; left-hand side) and light scattering (LS; right-hand side) detectors.

Table 2. Constants Required for the Calculation of Propagation Rate Coefficient Values from Pulsed Laser Polymerization/Size Exclusion Chromatography Data for the Homo- and Copolymerization of Styrene and Glycidyl Methacrylate (GMA)

monomer	monomer density ρ (g·mL^{-1}) = $\rho_o - bT$/°C	polymer dn/dc in THF (mL·g^{-1})	polymer Mark−Houwink parameters		
			K (dL·g^{-1})	a	ref
styrene	$0.91930 - 0.000665T^2$	0.180[2]	1.14×10^{-4}	0.716	*2*
GMA	$1.09428 - 0.001041T$[27]	0.093[a,30]	2.78×10^{-4}	0.537	*27*

[a] Measured in this work.

of GMA in the copolymer was calculated according to $F_1 = 5\ A_3/(5\ A_3 + 3\ A_2)$, where A_2 and A_3 are the peak areas of the phenyl and methyl protons, respectively. The polymer compositions estimated by the three methods were in good agreement, with the third method used in this work due to the distinct NMR resonance of the GMA methyl group even at low GMA mole fractions in the copolymer.

The propagation and depropagation kinetics of ST/GMA homo- and copolymerizations were determined by analyzing polymer MWDs of PLP samples as measured by SEC. SEC analyses were performed at 35 °C using a Waters 2960 separation module with Styragel packed columns HR 0.5, HR 1, HR 3, HR 4, and HR 5E (Waters Division Millipore). Tetrahydrofuran (THF) was used as the eluent at a flow rate of 1 mL/min and detection was provided by a Waters 410 differential refractometer (DRI detector) and a Wyatt Instruments Dawn EOS 690 nm laser photometer multiangle light scattering (LS) unit. Calibration for the DRI detector was established using 8 narrow PDI polystyrene standards over a molecular weight range of 890 to 3.55×10^5 g·mol^{-1} and MWDs of poly(GMA) were calculated by universal calibration using known Mark−Houwink parameters.[27] Composition-weighted universal calibration was used to calculate the MWDs of copolymers, as shown to be valid in previous studies.[2,28] The refractive index (dn/dc) of the polymer in THF is required to process the data from the LS detector and was measured by a Wyatt Optilab DSP refractometer at 35 °C and 690 nm calibrated with sodium chloride. Six samples of 1−20 mg·mL^{-1} were prepared in THF for each polymer and injected sequentially to construct a curve with slope dn/dc.

Results and Discussion

PLP/SEC experiments of GMA bulk and solution homopolymerization in xylene were conducted over an extended range of temperature. The full set of data and experimental conditions is summarized in Table S1, Supporting Information. PLP/SEC MWDs and corresponding derivative plots obtained for GMA bulk polymerization at 60−169 °C and a pulse repetition rate of 20 Hz are plotted in Figure 1. Good PLP structures can be observed for samples polymerized at temperatures up to 148 °C, with less distinct PLP structure found at higher temperature (169 °C) due to the increased influence of depropagation and other side reactions. Experiments at 50 Hz exhibited improved PLP structure and were used to verify k_p^{eff} measurements for this higher-temperature region.

GMA Propagation. Utilization of dual detectors (DRI and LS detector) provides an additional check in the accuracy of kinetic coefficients measured by the PLP/SEC technique. The DRI signal is proportional to polymer concentration, while the LS signal is proportional to the product of polymer concentration and molecular weight and thus is more sensitive to the existence of high-mass components present at low concentrations. Previous homopolymerization studies[2,29] indicated that good agreement between DRI and LS data could be expected if Mark−Houwink parameters used in universal calibration for DRI data and dn/dc value used in LS data analysis are correct. Table 2 lists all the constants required for calculation of GMA k_p from PLP/SEC data. The Mark−Houwink parameters of poly(GMA) were taken from literature[27] and the dn/dc value

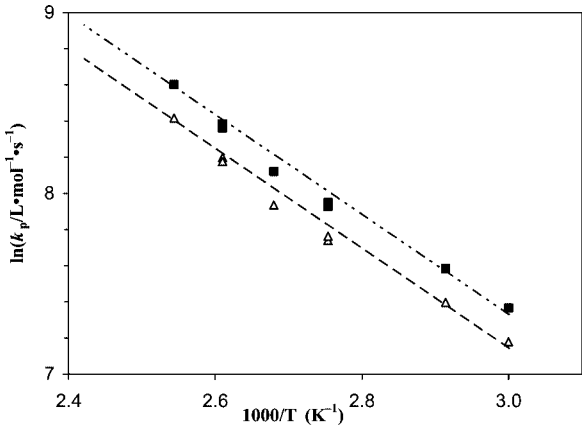

Figure 2. Propagation rate coefficients (k_p) measured by the pulsed laser polymerization/size exclusion chromatography (PLP/SEC) technique for glycidyl methacrylate (GMA) bulk homopolymerization between 60−120 °C (■, differential refractometer (DRI) detector; Δ, light scattering (LS) detector). The data are plotted against the IUPAC Arrhenius expression[31] (− • • −), and with the pre-exponential factor reduced by 17% (− − −) to fit the LS data.

was determined in this work. As shown in Figure 2, the k_p values calculated from the DRI detector using universal calibration are in very good agreement with the k_p expression fit to an IUPAC benchmark data set for GMA.[31] However, these values are higher than the k_p values calculated from the LS analysis, by a constant factor of 17%. We have more confidence in the LS estimates, as our measured dn/dc value of 0.093 mL•g^{-1} agrees well with that reported in literature,[30] with the mismatch between the two detectors perhaps due to error in the reported Mark−Houwink parameters used for DRI analysis. The LS data are well fit using the activation energy of 22.9 kJ•mol^{-1} from the IUPAC Arrhenius expression,[31] and lowering the frequency factor to 5.1 × 10^6 L•mol^{-1}•s^{-1}.

$$k_{p,GMA}/\mathrm{L\cdot mol^{-1}\cdot s^{-1}} = 5.1\times10^6 \exp(-2759/(T/K)) \quad (7)$$

Even with this adjustment, the propagation rate coefficient for GMA is still significantly higher than those for short-chain alkyl methacrylates such as BMA and methyl methacrylate.[32] For the remainder of this study, PLP/SEC results are calculated from MWDs measured via the LS detector, unless otherwise noted.

Depropagation Kinetics. The Arrhenius expression for k_{dep} was estimated by performing a linearized fit of ln(A_{dep}) and E_{dep} to eq 8.

$$\ln(k_{dep}) = \ln(A_{dep}) - (E_{dep}/R)(1/T) \quad (8)$$

where estimates for k_{dep} were calculated from a rearranged form of eq 2 for the 14 points collected between 138−175 °C, with eq 7 used to estimate k_p at these higher temperatures. Figure 3 plots the calculated k_{dep} values and the best fit to these data; the Arrhenius parameter estimates are compared to other methacrylates[8] in Table 3. The difference between E_p and E_{dep} is the heat of polymerization (ΔH_p); in ref 8 this value was estimated as −53.8 kJ•mol^{-1} for DMA from PLP/SEC results, in good agreement with the typically reported range of −50 to −55 kJ•mol^{-1} for methacrylates. The DMA estimate was then applied to the other methacrylates listed in Table 3 to estimate the reported E_{dep} values. While the estimated ($-\Delta H_p$) value of 48.5 kJ•mol^{-1} for GMA in this work is slightly lower, the k_{dep} data are also reasonable fit with E_{dep} set to 76.7 kJ•mol^{-1} ($-\Delta H_p$ = 53.8 kJ•mol^{-1}) and a higher value for ln(A_{dep}), as shown in Figure 3. Furthermore, the PLP/SEC k_p^{eff} data, plotted in Figure 4, are well fit using both sets of Arrhenius parameters for GMA depropagation. Note that this latter plot also contains results

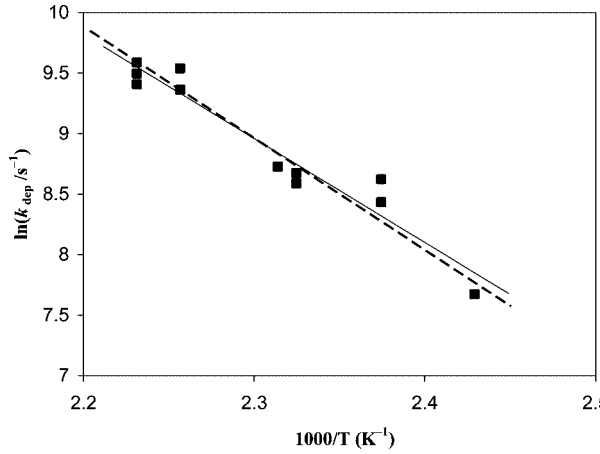

Figure 3. Depropagation rate coefficients, k_{dep}, estimated from k_p^{eff} pulsed laser polymerization/size exclusion chromatography (PLP/SEC) data for glycidyl methacrylate bulk polymerization between 138−175 °C. The solid line is the Arrhenius fit to the data points, while the dashed line is fit assuming a heat of polymerization of −53.8 kJ•mol^{-1}.

Table 3. Arrhenius Propagation and Depropagation Parameters for Glycidyl Methacrylate (GMA) and other Methacrylates[a]

monomer	ln(A_p) (L•mol^{-1}•s^{-1})	E_p (kJ•mol^{-1})	ln(A_{dep}) (s^{-1})	E_{dep} (kJ•mol^{-1})	ref
GMA	15.44	22.9	28.71	71.4	this work
			30.18	76.7	
DMA	14.67	20.8	29.48	74.6	*8*
BMA	14.79	21.8	30.19	75.6	*8*
CHMA	15.14	21.5	30.42	75.3	*8*
iBoMA	15.27	22.5	30.30	76.3	*8*
HPMA	14.29	20.8	30.59	74.6	*8*

[a] CHMA, cyclohexyl methacrylate; iBoMA, *iso*-bornyl methacrylate; HPMA, 2-hydroxypropyl methacrylate; DMA, dodecyl methacrylate; BMA, butyl methacrylate.

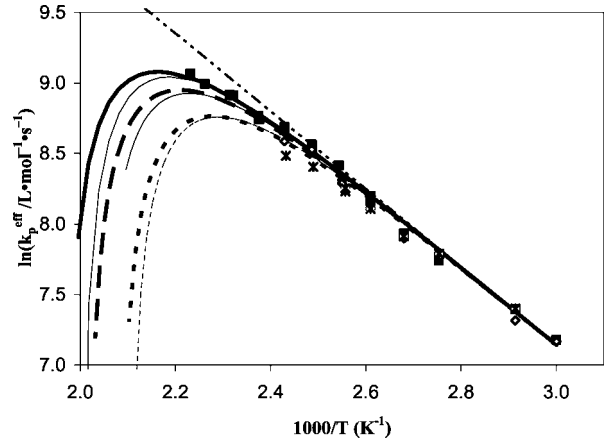

Figure 4. Glycidyl methacrylate (GMA) k_p^{eff} values measured in xylene solutions with [GMA] at 100% (v/v) (■), 75% (◇) and 50% (*) of the bulk value. Curves show predicted k_p (− • • −) and k_p^{eff} values for bulk monomer (—), 75% (− − −), and 50% (•••) solutions. Predictions of darker lines calculated with ln(A_{dep}/s^{-1}) = 28.71 and E_{dep} = 71.4 kJ•mol^{-1}; predictions of lighter lines calculated with ln(A_{dep}/s^{-1}) = 30.18 and E_{dep} = 76.7 kJ•mol^{-1} (see text for further details).

for solution polymerization in xylene solvent, with [GMA] reduced to 75 and 50% of bulk concentration; no significant solvent effects are observed. Thus, it can be concluded that while GMA may have a slightly lower value of ($-\Delta H_p$), it exhibits depropagation behavior consistent with DMA and other methacrylates.

Monomer Reactivity Ratios. As mentioned in the introduction, there is significant disagreement among the monomer

Table 4. Monomer Reactivity Ratios (r_{ST} and r_{GMA}) with 95% Confidence Intervals for Copolymerization of Styrene (ST) and Glycidyl Methacrylate (GMA)[a]

T (°C)	data points	r_{ST}	r_{GMA}
50	16	0.297 ± 0.010	0.492 ± 0.034
70	15	0.292 ± 0.016	0.513 ± 0.044
100	15	0.293 ± 0.009	0.536 ± 0.032
120	15	0.322 ± 0.018	0.519 ± 0.054
130	8	0.332 ± 0.067	0.516 ± 0.054
140	8	0.326 ± 0.060	0.497 ± 0.047
150−160	11	0.342 ± 0.021	0.511 ± 0.054
50−160	88	0.306 ± 0.007	0.508 ± 0.019

[a] Estimated by fitting copolymer composition data obtained at 50−160 °C.

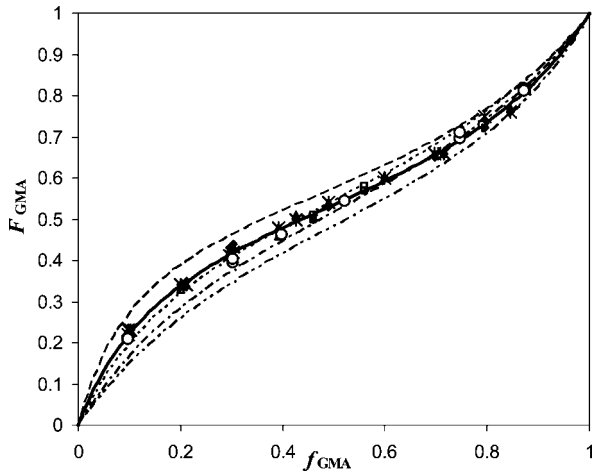

Figure 5. Copolymer composition data for low-conversion styrene/glycidyl methacrylate (GMA) copolymerization: mole fraction GMA in copolymer (F_{GMA}) vs mole fraction GMA in monomer mixture (f_{GMA}). The points are experimental data at different reaction temperatures: 50 (♦), 70 (Δ), 100 (*), 130 (□), 140 (+), and 160 °C (○). The curves are predictions of Mayo−Lewis equation using literature monomer reactivity ratios from: Beuermann et al. (—),[14] Soundararajan et al. (— • • —),[13] Brar et al. (— • —),[12] Wolf et al. (— — —),[11] and Dhal (•••).[10] See Table S2, Supporting Information for copolymer composition and conversion data.

reactivity ratios reported in literature. Furthermore, little experimentation has been done at temperatures >100 °C, the range of interest for solution acrylic resins. Thus, low conversion PLP experiments of ST/GMA copolymerization were conducted over an extended temperature range (50−160 °C). While not required for composition analysis, the use of the PLP setup is convenient, as the use of the photoinitiator allows the cell to be heated and stabilized at reaction temperature without any polymerization occurring. Monomer reactivity ratios, estimated using the nonlinear parameter estimation capabilities of the computer package Predici by fitting of the Mayo−Lewis equation to the experimental mole fraction of GMA in copolymer (F_{GMA}) data obtained at each temperature, as well as the entire 50−160 °C data set, are listed in Table 4. No significant variation with temperature is observed for r_{GMA}, while r_{ST} possibly shows a slight increase with temperature. The entire data set is well fit with temperature-independent values of $r_{ST} = 0.31$ and $r_{GMA} = 0.51$, in agreement with the values of $r_{ST} = 0.29$ and $r_{GMA} = 0.48$ reported by Beuermann et al.[14] The measured copolymer composition data and the predictions of Mayo−Lewis equation using the monomer reactivity ratios from literature (Table 1) are plotted in Figure 5.

Although GMA and alkyl methacrylates (e.g., BMA, DMA and methyl methacrylate (MMA)) exhibit the same general behavior when copolymerized with styrene, the functional epoxy group of GMA monomer does have a significant influence on its copolymer composition and copolymerization kinetics. Table 5 compares the monomer reactivity ratios for ST/GMA, ST/BMA, ST/DMA, and ST/MMA systems, and the associated plots of copolymer composition versus methacrylate mole fraction (f_{mac}) are shown as Figure 6. The reactivity ratio values and the composition plots are quite similar for copolymerization of the three alkyl methacrylates. However, the formation of GMA-enriched copolymer (relative to the alkyl methacrylates) occurs at low values of f_{mac}, resulting in a reduced r_{ST} estimate for ST/GMA. This difference cannot be attributed to the higher k_p of GMA, as DMA also homopolymerizes significantly more quickly than MMA or BMA (see Table 5). It is not clear why

Table 5. Monomer Reactivity Ratios (r_{ST} and r_{mac}) for Methacrylate (mac)/Styrene (ST) Copolymerizations

	ST/GMA[this work]	ST/BMA[2]	ST/MMA[28]	ST/DMA[33]
r_{ST}	0.31	0.61	0.489	0.57
r_{mac}	0.51	0.42	0.493	0.45
$k_{p,mac}$[a]	999	756	649	1012

[a] In L·mol^{-1}·s^{-1} at 50 °C. GMA k_p value from eq 7, and other values from ref 32. GMA, glycidyl methacrylate; BMA, butyl methacrylate; MMA, methyl methacrylate; DMA, dodecyl methacrylate.

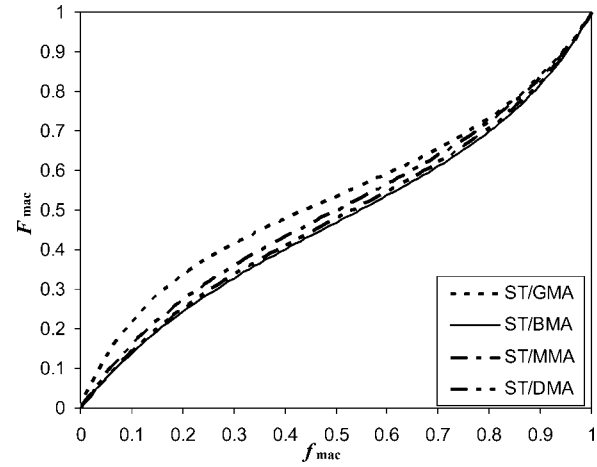

Figure 6. Methacrylate mole fraction in copolymer (F_{mac}) vs its mole fraction in monomer mixture (f_{mac}) for styrene (ST)/glycidyl methacrylate (GMA), ST/butyl methacrylate (BMA), ST/dodecyl methacrylate (DMA), and ST/methyl methacrylate (MMA) systems, calculated using the monomer reactivity ratios in Table 5.

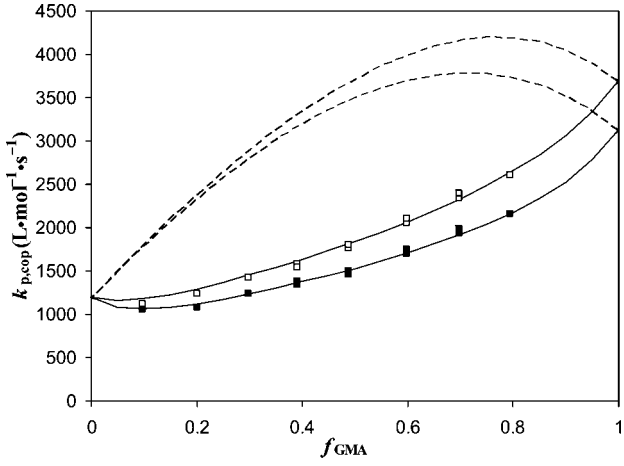

Figure 7. Experimental copolymer-averaged propagation rate coefficients ($k_{p,cop}$) styrene/glycidyl methacrylate (GMA) data vs GMA monomer mole fraction, as obtained by pulsed laser polymerization/size exclusion chromatography (PLP/SEC) at 100 °C (□, differential refractometer (DRI) data; ■, light scattering (LS) data). Terminal model predictions are indicated by dashed lines (— — —); penultimate model fits (—) calculated with radical reactivity ratios $s_{ST} = 0.32$ and $s_{GMA} = 1.37$ for DRI data, and $s_{ST} = 0.28$ and $s_{GMA} = 1.05$ for LS data.

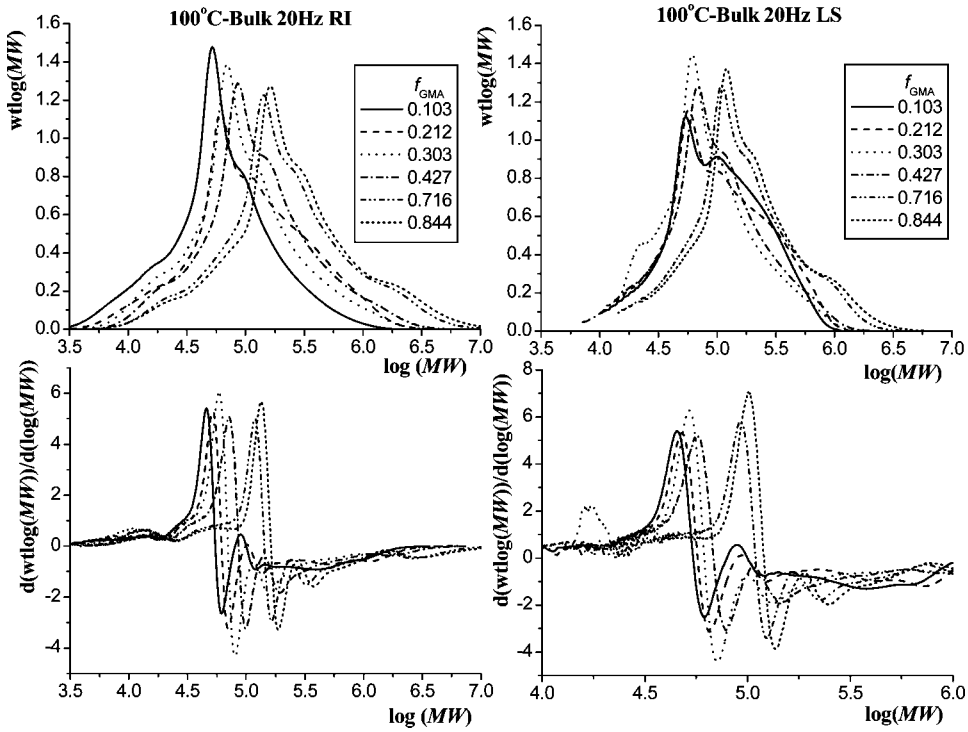

Figure 8. Molecular weight distributions (top) and corresponding first derivative (bottom) plots obtained for styrene (ST)/glycidyl methacrylate (GMA) copolymer produced by pulsed laser polymerization (PLP) at 100 °C and 20 Hz, as measured by differential refractometer (DRI; left-hand side) and light scattering (LS; right-hand side) detectors.

Table 6. Radical Reactivity Ratios (s_{ST} and s_{GMA}) with 95% Confidence Intervals for Styrene (ST) and Glycidyl Methacrylate (GMA) Copolymerization[a]

SEC analysis	T (°C)	data points	$k_{p,ST}$ (L·mol^{-1}·s^{-1})	$k_{p,GMA}$ (L·mol^{-1}·s^{-1})	s_{ST}	s_{GMA}
DRI	50−140	84	IUPAC[37]	IUPAC[31]	0.323 ± 0.014	1.369 ± 0.466
LS	50−140	84	IUPAC[37]	eq 7	0.278 ± 0.009	1.046 ± 0.228

[a] Estimated from the implicit penultimate unit model fit to experimental $k_{p,cop}$ data obtained at 50−140 °C.

GMA is more active toward styrene radicals than the other methacrylates. It has been observed that the carbonyl IR peak for GMA is shifted to a lower wavelength by 5 cm^{-1} relative to MMA, and that a shift in this direction correlates with higher monomer activity.[34] A computational study to investigate the difference in reactivity between functional and alkyl methacrylates is underway; calculations show that the charges over the transition state are more uniformly distributed for GMA relative to BMA, increasing its relative reactivity toward the ST radical.[35]

Radical Reactivity Ratios. With monomer reactivity ratios and homopropagation rate coefficients now known, the next step is to determine whether or not the IPUE propagation model is required to represent copolymer-averaged propagation rate, $k_{p,cop}$. This treatment is needed for copolymerization of styrene with alkyl methacrylates,[2,28,33] but has not been studied for functional monomers such as GMA. PLP experiments were carried out at 20 Hz for ST and GMA monomer mixtures of varying composition containing 3−5 mmol·L^{-1} DMPA photoinitiator at temperatures ranging from 50 to 140 °C. The full set of data and experimental conditions can be found in Table S2, Supporting Information. The data set obtained at 100 °C is shown in Figure 7, with Figure 8 containing the corresponding MWDs and derivative plots. Clear characteristic PLP structures were obtained, with MWD and the position of the maxima in the first derivative plots shifting toward higher molecular weight with increasing GMA mole fraction. The DRI data were processed assuming a composition-weighted average of homopolymer calibrations and LS data treated using a weighted average of poly(GMA) and poly(ST) dn/dc values.[2] As found for GMA homopolymer, there is a mismatch between the DRI data and LS data for copolymerization that is maximum for GMA homopolymer and diminishes with increasing ST content in the copolymer (see Figure 7). Despite this uncertainty, it is clear that the ST/GMA $k_{p,cop}$ values deviate significantly, by as much as a factor of 2, from terminal model predictions, and that the behavior is well represented with the IPUE model of copolymerization propagation kinetics.

As done for the ST/BMA system,[2] the combined $k_{p,cop}$ data set from 50 to 140 °C was used to estimate the radical reactivity ratios (s_{ST} and s_{GMA}), to reduce the variability in the estimates obtained from fitting fewer points at each temperature.[19] The radical reactivity ratios were estimated separately for the DRI and LS data, with eq 7 used for $k_{p,GMA}$ for fitting of the LS data, and the IUPAC homopropagation rate coefficients[31] used for fitting of the DRI data set. For both cases the monomer reactivity ratios $r_{GMA} = 0.51$ and $r_{ST} = 0.31$ were used, as was the IUPAC recommended expression for $k_{p,ST}$.[37] The resulting s values, estimated using the nonlinear parameter estimation capabilities of the computer package Predici, are summarized in Table 6. While there are differences in the s values estimated from the DRI and LS $k_{p,cop}$ values, they are relatively small and reflect the uncertainty in SEC calibration. As also found for ST/BMA, the uncertainty is higher for the s_{GMA} estimate. The excellent fit of the IPUE model to the LS $k_{p,cop}$ data set over the complete temperature range (from 50 to 140 °C) with $s_{ST} = 0.28$ and $s_{GMA} = 1.05$ is illustrated in Figure 9. The ability of temperature-independent radical reactivity ratios to represent data over a wide temperature range was also found for ST/BMA.[2] As pointed out by Coote et al.,[36] this result does

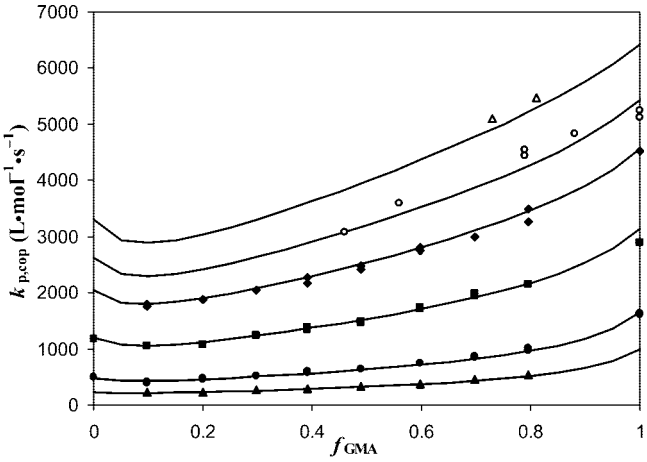

Figure 9. Experimental copolymerization propagation rate coefficient $k_{p,cop}$ data from light scattering (LS) detector vs glycidyl methacrylate (GMA) monomer mole fraction, as obtained by pulsed laser polymerization (PLP)/size exclusion chromatography (SEC) at 50 (▲), 70 (●), 100 (■), 120 (♦), 130 (○), and 140 °C (Δ). Penultimate model predictions calculated with radical reactivity ratios $s_{ST} = 0.28$ and $s_{GMA} = 1.05$ are indicated by lines.

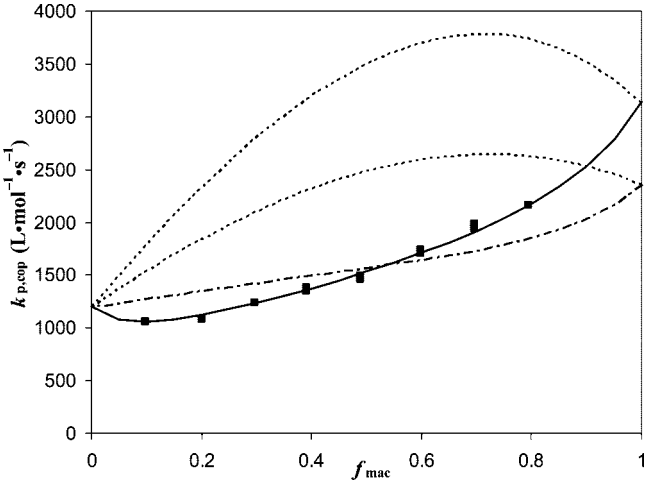

Figure 10. Comparison between copolymerization propagation rate coefficient $k_{p,cop}$ vs methacrylate monomer mole fraction (f_{mac}) of styrene (ST)/glycidyl methacrylate (GMA) and ST/butyl methacrylate (BMA) systems at 100 °C. Penultimate model predictions for ST/GMA (—) calculated with radical reactivity ratios $s_{ST} = 0.28$ and $s_{GMA} = 1.05$, and ST/BMA (— • —) calculated with $s_{ST} = 0.44$ and $s_{BMA} = 0.62$. The dotted lines (•••) are the terminal model predictions.

not prove the absence of temperature effects on penultimate kinetics, but simply indicates that they cannot be found within the accuracy of the data set.

The IPUE $k_{p,cop}$ kinetics of the ST/GMA system is compared to that of ST/BMA at 100 °C in Figure 10. The two systems show the same general behavior, with differences in shape observed at lower methacrylate mole fractions. For f_{GMA} less than 0.2, $k_{p,cop}$ decreases to a value slightly lower than that of $k_{p,ST}$, indicating that the GMA unit in the penultimate position to styrene reduces monomer addition rate to a greater extent than BMA. Also, the difference between the terminal and penultimate model predictions for ST/GMA copolymerization is larger than that found for ST/BMA, emphasizing the importance of considering penultimate effects for this system.

Conclusions

Free radical copolymerization kinetics of ST and GMA have been investigated over an extended temperature range (50−140 °C). GMA exhibits depropagation similar to other methacrylates at elevated temperatures, with the Arrhenius expression for k_{dep} estimated from PLP/SEC data. Monomer and radical reactivity ratios for ST/GMA copolymerization show a negligible temperature dependency between 50−140 °C, as also found for ST/BMA.[2] The "implicit penultimate unit effect" model gives a good representation of both copolymer composition and measured $k_{p,cop}$ data. Compared to the ST/BMA system, GMA monomer is more active toward styrene radicals and the GMA unit in penultimate position of styrene radicals reduces $k_{p,cop}$ to a larger degree. High temperature semibatch copolymerization of ST and GMA is underway, and the experimental data will be compared to the predictions of our previous mechanistic model[4] using the coefficients and mechanisms determined in this work.

Acknowledgment. We thank E. I. du Pont de Nemours and Co. and the Natural Sciences and Engineering Research Council of Canada for financial support of this work.

Supporting Information Available: Figure S1 indicates proton NMR peak assignments, and Tables S1 and S2 summarize detailed PLP/SEC results for GMA homopolymerization and GMA/ST copolymerization. This material is available free of charge via the Internet at http://pubs.acs.org.

References and Notes

(1) Grady, M. C.; Simonsick, W. J., Jr.; Hutchinson, R. A. *Macromol. Symp.* **2002**, *182*, 149–168.
(2) Li, D.; Li, N.; Hutchinson, R. A. *Macromolecules* **2006**, *39*, 4366–4373.
(3) Li, D.; Hutchinson, R. A. *Macromol. Symp.* **2006**, *243*, 24–34.
(4) Wang, W.; Hutchinson, R. A. *Macromol. React. Eng.* **2008**, *2*, 199–214.
(5) Ghosh, S.; Krishnamurti, N. *Eur. Polym. J.* **2000**, *36*, 2125–2131.
(6) Dela Fuente, J. D.; Cañamero, P. F.; Fernández-García, M. *J. Polym. Sci., Part A: Polym. Chem.* **2006**, *44*, 1807–1816.
(7) Bywater, S. *Trans. Faraday Soc.* **1955**, *51*, 1267–1273.
(8) Hutchinson, R. A.; Paquet, D. A., Jr.; Beuermann, S.; McMinn, J. H. *Ind. Eng. Chem. Res.* **1998**, *37*, 3567–3574.
(9) Li, D.; Leiza, J. R.; Hutchinson, R. A. *Macromol. Theory Simul.* **2005**, *14*, 554–559.
(10) Dhal, P. K. *J. Macromol. Sci. Chem.* **1986**, *A23*, 181–187.
(11) Wolf, A.; Bandermann, F.; Schwede, C. *Macromol. Chem. Phys.* **2002**, *203*, 393–400.
(12) Brar, A. S.; Yadav, A.; Hooda, S. *Eur. Polym. J.* **2002**, *38*, 1683–1690.
(13) Soundararajan, S.; Reddy, B. S. R.; Rajadurai, S. *Polymer* **1990**, *31*, 366–370.
(14) Beuermann, S.; Buback, M.; Jürgens, M. *Ind. Eng. Chem. Res.* **2003**, *42*, 6338–6342.
(15) Fukuda, T.; Ma, Y.; Inagaki, H. *Macromolecules* **1985**, *18*, 17–26.
(16) Davis, T. P. *J. Polym. Sci., Part A: Polym. Chem.* **2001**, *39*, 597−603.
(17) Coote, M. L.; Davis, T. P. *Prog. Polym. Sci.* **1999**, *24*, 1217−1251.
(18) Buback, M.; Müller, E. *Macromol. Chem. Phys.* **2007**, *208*, 581–593.
(19) Hutchinson, R. A.; McMinn, J. H.; Paquet, D. A.; Beuermann, S.; Jackson, C. *Ind. Eng. Chem. Res.* **1997**, *36*, 1103–1113.
(20) Buback, M.; Garcia-Rubio, L. H.; Gilbert, R. G.; Napper, D. H.; Guillot, J.; Hamielec, A. E.; Hill, D.; O'Driscoll, K. F.; Olaj, O. F.; Shen, J.; Solomon, D.; Moad, G.; Stickler, M.; Tirrell, M.; Winnik, M. A. *J. Polym. Sci., Part C: Polym. Lett.* **1988**, *26*, 293–297.
(21) Buback, M.; Gilbert, R. G.; Russell, G. T.; Hill, D. J. T.; Moad, G.; O'Driscoll, K. F.; Shen, J.; Winnik, M. A. *J. Polym. Sci., Polym. Chem. Ed.* **1992**, *30*, 851–864.
(22) Coote, M. L.; Zammit, M. D.; Davis, T. P. *Trends Polym. Sci.* **1996**, *4*, 189–196.
(23) Davis, T. P. *J. Photochem. Photobiol., A* **1994**, *77*, 1–7.
(24) Van Herk, A. M. *J. Macromol. Sci., Part C: Rev. Macromol. Chem. Phys.* **1997**, *C37*, 633–648.
(25) Van Herk, A. M. *Macromol. Theory Simul.* **2000**, *9*, 433–441.
(26) Beuermann, S.; Buback, M. *Prog. Polym. Sci.* **2002**, *27*, 191–254.
(27) Hutchinson, R. A.; Beuermann, S.; Paquet, D. A., Jr.; McMinn, J. H.; Jackson, C. *Macromolecules* **1998**, *31*, 1542–1547.
(28) Coote, M. L.; Zammit, M. D.; Davis, T. P.; Willett, G. D. *Macromolecules* **1997**, *30*, 8182–8190.

(29) Li, N.; Cho, A. S.; Broadbelt, L. J.; Hutchinson, R. A. *Macromol. Chem. Phys.* **2006**, *207*, 1429–1438.
(30) Hild, G.; Lamps, J. P.; Rempp, P. *Polymer* **1993**, *34*, 2875–2882.
(31) Beuermann, S.; Buback, M.; Davis, T. P.; Garcia, N.; Gilbert, R. G.; Hutchinson, R. A.; Kajiwara, A.; Kamachi, M.; Lacik, I.; Russell, G. T. *Macromol. Chem. Phys.* **2003**, *204*, 1338–1350.
(32) Beuermann, S.; Buback, M.; Davis, T. P.; Gilbert, R. G.; Hutchinson, R. A.; Kajiwara, A.; Klumperman, B.; Russell, G. T. *Macromol. Chem. Phys.* **2000**, *201*, 1355–1364.
(33) Davis, T. P.; O'Driscoll, K. F.; Piton, M. C.; Winnik, M. A. *Macromolecules* **1990**, *23*, 2113–2119.
(34) Woecht, I.; Schmidt-Naake, G.; Beuermann, S.; Buback, M.; Garcia, N. *J. Polym. Sci., Part A: Polym. Chem.* **2008**, *46*, 1460–1469.
(35) Dossi, M.; Moscatelli, D. *Politecnico Milano*, **2008**, unpublished work.
(36) Coote, M. L.; Johnston, L. P. M.; Davis, T. P. *Macromolecules* **1997**, *30*, 8191–8204.
(37) Buback, M.; Gilbert, R. G.; Hutchinson, R. A.; Klumperman, B.; Kuchta, F. D.; Manders, B. G.; O'Driscoll, K. F.; Russell, G. T.; Schweer, J. *Macromol. Chem. Phys.* **1995**, *196*, 3267–3280.

MA801435T